06

Fabrication of B_4C/TiB_2 composite ceramics using boron carbide reduction

© T.S. Gudyma,[1] R.R. Khabirov,[1] Yu.L. Krutskii,[1] N.Yu. Cherkasova,[1] A.G. Bannov,[1] A.O. Semenov[2]

[1] Novosibirsk State Technical University,
630073 Novosibirsk, Russia
[2] Tomsk Polytechnic University,
634050 Tomsk, Russia
e-mail: gudymatan@mail.ru

Received October 4, 2024
Revised October 4, 2024
Accepted October 4, 2024

B_4C/TiB_2 composite ceramics were fabricated by pressing B_4C/TiB_2 powder mixtures, as well as by reaction pressing. The TiB_2 phase content was 10–30 mol%. It was revealed that increasing the TiB_2 additive content reduces open porosity and increases the relative density of composite ceramics. Visual analysis showed that simultaneous boron carbide synthesis and hot pressing makes it possible to obtain a $B_4C/10$ mol% TiB_2 material with uniformly distributed TiB_2 grains throughout the B_4C phase. The microhardness and fracture toughness of such a material were 41.1 GPa and 4.4 MPa $\cdot$ $m^{0.5}$, respectively. The relative density was 99.9%. In the case of hot pressing of a pre-synthesized powder mixture, similar results were achieved with a higher content of the modifying additive, corresponding to 30 mol.% diboride. It has been shown that composite ceramics containing 30 mol% TiB_2 have a higher thermal neutron absorption cross section compared to unmodified ceramics.

Keywords: titanium diboride, nanofibrous carbon, boron carbide, refractory compounds.

DOI: 10.61011/TP.2025.02.60825.283-24

Introduction

Interest in ceramic materials with high impact resistance has been growing over the past years. Such materials include B_4C. B_4C features such properties as high hardness (to 50 GPa) and low density (2.52 g/cm^3). B_4C is used as an absorbing material in nuclear reactor monitoring and protection systems. Due to high content of boron, such ceramics has a high thermal neutron absorption cross-section. Limited use of B_4C in ceramic production results from its insufficient sintering capability and relatively low fracture toughness [1,2].

Addition of transition metal diborides is one of the methods for solution of the above-mentioned problem [3–5]. Some studies used TiB_2 as an additive [6–8]. This material features high melting temperature ($\sim 3200^\circ$C) and microhardness (25–34 GPa) [9,10].

Most studies devoted to making the B_4C/TiB_2 ceramics employ ready-to-use B_4C and TiB_2 powders [11–13]. However, high-purity transition metal diborides are very expensive. Therefore, process solutions using cheaper reagents, e.g. oxides, are being extensively developed for boron carbide synthesis of the additive modifying phase during compaction in accordance with reaction (1) [14]:

$$(1+x)B_4C + 2xTiO_2 + 3xC = B_4C + 2xTiB_2 + 4xCO. \quad (1)$$

For example, in [15], B_4C–20 mol% TiB_2 composite ceramics was made by the combination of boron carbide synthesis and hot pressing (HP). B_4C, TiO_2 powders and carbon black were used as reagents. The process was performed at 2000°C and 60 MPa during 60 min. Ceramics made by both methods had a strength of 866 MPa and quite moderate fracture resistance 3.2 MPa $\cdot$ $m^{0.5}$. Note that carbon black is used as carbon material in most of works devoted to the boron carbide synthesis of B_4C/TiB_2 composite materials [16,17]. Relatively low specific surface ~ 75 m^2/g is the disadvantage of this reagent. There are materials with more developed specific surface area. For example, carbon nanofibers (~ 150 m^2/g) and activated charcoals (~ 2000 m^2/g). Activated charcoals have instable composition and may contain a considerable amount of impurities. Ash content of such carbons is about 5%. Activated charcoals are characterized by the presence of micropores, while carbon nanofibers are characterized by mesopores that facilitate higher reactivity of a carbon material. This study uses carbon nanofibers as a carbon material. Methane, an easily available raw material, is used for carbon nanofiber manufacturing. In addition, production of carbon nanofibers is currently treated as a promising technique for associated petroleum gas decomposition. Extension of the sales market for this material, in particular, for making hard-melting ceramics, facilitates carbon footprint reduction in the domestic oil industry.

The objective of this study was to examine the properties of B_4C/TiB_2 composite ceramics made through the boron carbide reduction process. Hot pressing of a pre-synthesized batch and reactive pressing of ceramics were performed.

Marking of the B_4C/TiB_2 ceramic samples

Sample marking	TiB content$_2$, mol%	synthesis technique B_4C/TiB_2
T0HP	0	Preliminary synthesis in furnace
T10sHP	10	Preliminary synthesis in furnace
T20sHP	20	Preliminary synthesis in furnace
T30sHP	30	Preliminary synthesis in furnace
T10HP	10	In press matrix

1. Experimental

The following reagents were used for the synthesis of B_4C/TiB_2 composite materials: B_4C powder (purity 98.5 mass%, $d_{av} = 2.1\,\mu$m) synthesized from carbon nanofibers and B powder [18]; commercial TiO_2 (purity 99.0 mass%, $d_{av} = 1.0\,\mu$m, PROMKhIMPERM, Russia); carbon nanofibers (carbon content 99.0 mass%, $d_{av} = 3.9\,\mu$m) [19].

Some ceramic samples were made by compaction of ready-to-use B_4C/TiB_2 powder mixtures. The mixtures were pre-synthesized in accordance with reaction (1) in an indirect-heating induction furnace at 1650°C using a procedure described in [20,21]. The other part of ceramic samples was made by the reactive pressing technique also in accordance with reaction (1), i.e. the synthesis took place directly during compaction in the press matrix. The batch composition corresponded to the content of TiB_2 0−30%. Before pressing, the batch was stirred and milled in the AGO-2S planetary ball mill with an acceleration of 20 g for 5 min.

Compact samples were prepared by the HP method using a compact laboratory hot press (Scientific Instrumentation Design and Technology Institute, Siberian Branch, RAS, Russia). Maximum pressing temperature was 2000°C at 25 MPa. Heating was performed at a rate of 50°C/min until 1500°C, then at a rate of 35°C/min until the maximum temperature was reached. Temperature measurement error was 1% of the measured value. Holding time at the maximum parameters was 10 min. Argon was used to maintain inert atmosphere in the matrix.

Ceramic sample marking is shown in the table.

Diffraction patterns of the samples were made using the ARL X'TRA („Thermo Fisher Scientific (Ecublens) SARL“, Switzerland) diffractometer with a $\theta-\theta$-goniometer. The Williamson−Hall method was used to calculate the mean size of B_4C phase crystallites.

The relative density was measured by hydrostatic weighing in accordance with GOST 2409-2014 [22].

Microstructural examination of polished ceramic samples and fracture surface was performed using the EVO 50 („Carl Zeiss“, Germany) scanning-electron microscope equipped with the INCA X-ACT energy-dispersive X-ray spectroscopy module. Grain and aggregate sizes were measured using JMicroVision software.

Ceramics hardness and fracture toughness were measured using the 402MVD („Wolpert Group“, Netherlands) Vickers microhardness tester. Hardness was measured in accordance with GOST 2999-75 [23] at the indenter loading of 500 g. Fracture toughness was measured by indentation with loading set to 5 kg. Fracture toughness was calculated using equation (2) [24]:

$$K_{IC} = 0.048\left(\frac{l}{a}\right)^{-0.5}\left(\frac{H_v}{E\beta}\right)^{-0.4}\frac{H_v a^{0.5}}{\beta}, \qquad (2)$$

where a is the indentation semidiagonal, [μm]; H_v is the hardness, [GPa]; l is the fracture length, [μm]; β is the constant ($\beta = 3$); E is the longitudinal modulus of elasticity, [GPa].

Absorbing capacity of ceramics was evaluated by determining the thermal neutron flux density variation in the 4 mm test sample followed by the calculation of macroscopic absorption cross-section of the material. Measurements were performed using the MKS-AT1117M (NPP Doza, Russia) multipurpose dosimeter-radiometer and the BDKN-03 (ATOMTEKh,Belarus) detecting unit. Neutron flux accumulation was performed during 0.5 min. Thermal neutron absorption cross-section ($\Sigma_a, \mathrm{cm}^{-1}$) was calculated using the neutron flux density attenuation law:

$$F = F_0\, e^{-\Sigma_a r}, \qquad (3)$$

where F is the thermal neutron flux density after passing through the sample, [n/(cm$^2\cdot$ s)]; F_0 is the thermal neutron flux density without a sample, [n/(cm$^2\cdot$ s)]; r is the absorbing material thickness, [cm].

2. Findings and discussion

Results of the study of TiB_2 additive and pressing technique effects on the relative density and open porosity of ceramics are shown in Figure 1.

Among the modified ceramics samples, a B_4C/10 mol% TiB_2 sample made by reactive hot pressing demonstrated the highest relative density (99.90%) together with low open porosity (0.07%). The obtained data proves the assumption that the effective composite ceramics compaction is achieved by combining the synthesis and compaction processes [17]. In the samples made by hot pressing of the pre-synthesized B_4C/TiB_2 mixture containing 10−20 mol% of modifying additive, low relative densities were recorded. This may indicate insufficient activity of diffusion processes that take place in the batch during the induction furnace synthesis.

To determine the extent of boron carbide reduction reaction during reactive hot pressing, X-ray diffraction analysis of sample T10HP was performed (Figure 2). This sample was characterized by the highest compaction.

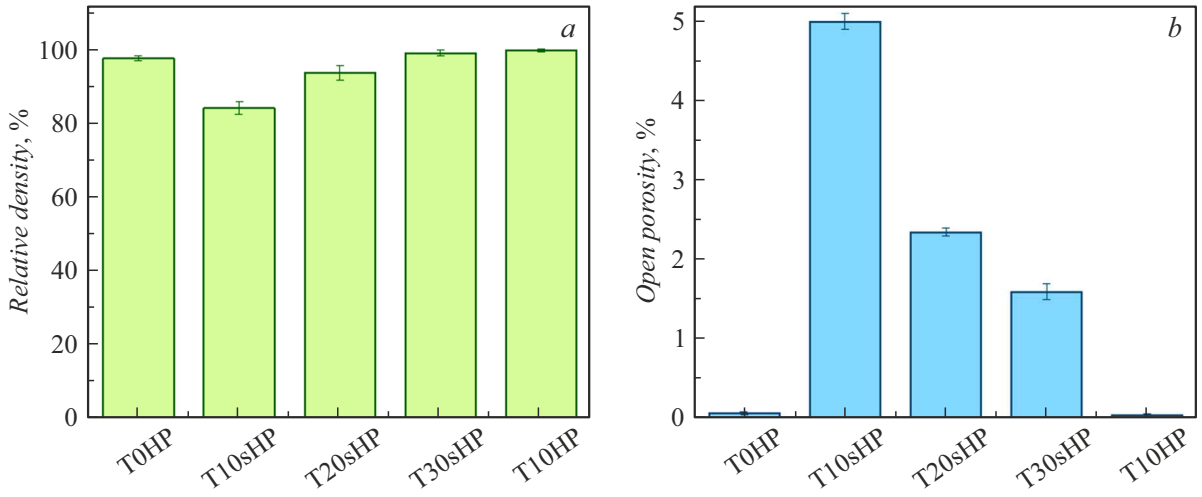


Figure 1. Relative density (a) and open porosity (b) measurements.

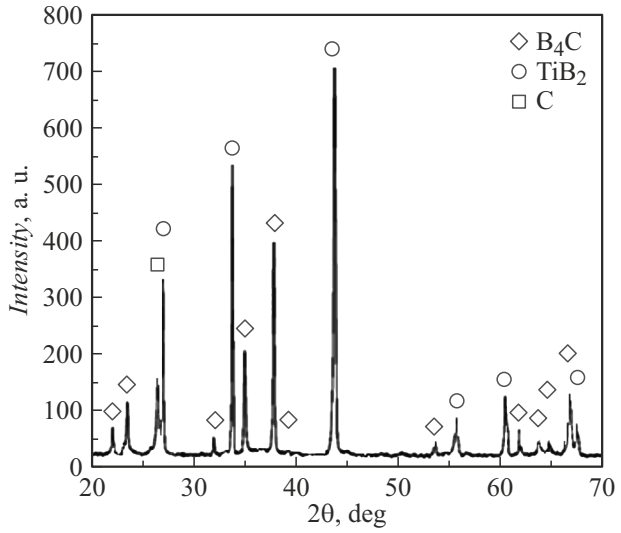


Figure 2. Diffraction pattern of the $B_4C/10\,mol\%\,TiB_2$ sample, reactive hot pressing method.

The presence of C was detected in the sample besides the B_4C and TiB_2 target phases. For charging the batch into the die mold, the plunger surface in contact with the sample is covered with graphite paper. Carbon included in the graphite paper could penetrate the sample and affect the XPA results. Mole phase ratio $B_4C:TiB_2:C$ was 87:9:4.

Grain size and the type of distribution of the modifying additive phase in the principal phase volume were determined by the microstructural analysis of ceramics. The mean grain size of the TiB_2 phase for samples T10sHP, T20sHP, T30sHP and T10HP was 1.0, 1.4, 7.0, 0.9 μm, respectively. The mean grain size of TiB_2 increase with the modifying additive fraction in the ceramics. The smallest grain size of TiB_2 is typical of the sample synthesized directly during HP and characterized by the maximum compaction. Note that the mean crystallite size of the B_4C phase for this sample was 42 nm, which was smaller than that for the sample without additives (83 nm). This may indicate that the introduction of the secondary phase results in the decrease of the B_4C grain size. This effect may be explained by the difference in linear thermal expansion coefficients of phases included in the ceramics: $4.5 \cdot 10^{-6}\,K^{-1}$ for B_4C and $4.6 \cdot 10^{-6}\,K^{-1}$ for TiB_2 [25].

Figure 3 shows the microimages of sample T10HP made by combining the ceramics synthesis and compaction. The images were made in the secondary electron recording mode. Sufficiently uniform distribution of the modifying additive phase in the ceramics volume may be observed. Spalling may be also observed in the microphotographs.

Figure 4 shows the microphotograph of sample T30sHP that was made by HP of the pre-synthesized batch and has high relative density similar to sample T10HP.

This sample is characterized by sufficiently large modifying phase aggregates larger than 100 μm and pores up to 15 μm. Pores and spalling in the material structure may indicate low binding strength of the grain boundaries.

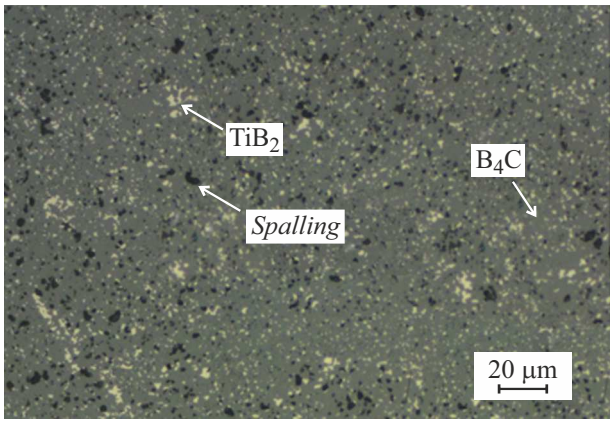


Figure 3. Microstructure of the $B_4C/10\,mol\%\,TiB_2$ ceramics, reactive hot pressing.

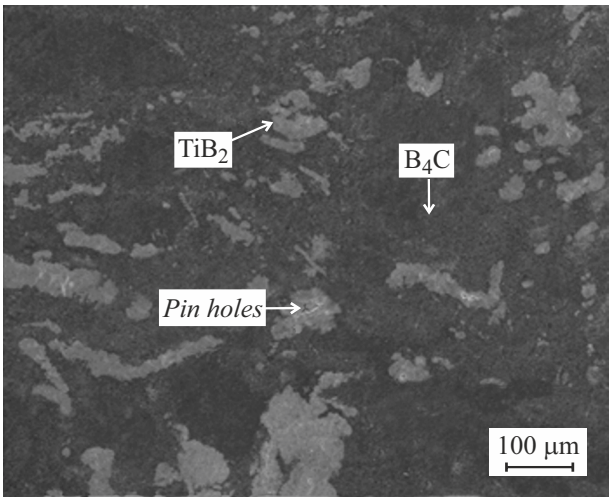


Figure 4. Microstructure of the $B_4C/30\,mol\%\,TiB_2$ ceramics made by HP of the pre-synthesized batch.

Fracture surface examination of the ceramic samples showed the difference in the type of fracture of the B_4C and TiB_2 phase grains (Figure 5).

It can be seen that intragranular type of fracture is observed for the B_4C phase, while intergranular fracture is observed for the TiB_2 phase. This suggests that the fracture propagating over the volume of the principal phase changes its direction when it contacts the TiB_2 grains and its energy will decrease gradually (Figure 6).

Figure 7 shows the microhardness and fracture toughness measurements of the ceramic samples.

Note that microhardness for all samples containing the diboride additive was lower than for additive-free sample T0HP. This is probably due to the fact that TiB_2 has lower microhardness than the B_4C phase. Introduction of a phase with lower microhardness facilitates the decrease in the total hardness of the composite material.

Sample T10HP made by reactive hot pressing demonstrated the highest microhardness ($41 \pm 2\,GPa$). Microhardness of samples made by pressing the pre-synthesized batch was much lower. The highest fracture toughness ($4.8 \pm 0.2\,MPa \cdot m^{0.5}$) was typical of sample T30sHP made by hot pressing of the pre-synthesized mixture. Note that the samples made by combining the synthesis and pressing were just slightly inferior to this sample, whereas the content of diboride in them was lower. Thus, reactive pressing of the B_4C/TiB_2 ceramics is more reasonable.

As long as boron carbide is used in absorbers included in reactor absorber rods, it is important to evaluate the thermal neutron absorption cross-section variation by the boron carbide ceramics when new phases are introduced. For unmodified boron carbide, the thermal neutron absorption cross-section was $3.5 \pm 0.1\,cm^{-1}$. Experiments carried out to evaluate the neutron absorption capacity of modified sample T30sHP showed that the neutron flux density decreased from 289.7 to $58.4\,n/(cm^2 \cdot s)$ during passing through the ceramic layer. The macroscopic thermal neutron absorption cross-section calculated using equation (3) is $5.4 \pm 0.4\,cm^{-1}$ in this case, which is higher than that for pure B_4C. This suggests that introduction of the additive doesn't give rise to a decrease in the absorbing capacity of the material, but rather facilitates the increase in the absorbing capacity. This in turn might make it possible to reduce the absorbing material thickness in reactor absorber rods. Equation (3) was used to determine the change of density of thermal neutron flux going out of the sample during radiation depending on the ceramics thickness. It was considered that the flux density in water-cooled reactors before passing through the absorber rods was $1 \cdot 10^{13}\,n/(cm^2 \cdot s)$. The obtained dependence (Figure 8) demonstrates that, when the material thickness is up to $\sim 1.4\,cm$, ceramics with diboride additive absorbs a large amount of neutrons.

Nuclear reactors use 0.76 cm absorber elements [26]. Therefore, absorbing capacity evaluation of materials with such thickness is of interest. Density of neutron flux during passing through the 0.76 cm pure and modified boron carbide samples was calculated. It was equal to $1.6 \cdot 10^{11}$ and $6.9 \cdot 10^{11}\,n/(cm^2 \cdot s)$ for the modified and unmodified ceramics, respectively. The calculation data suggests that

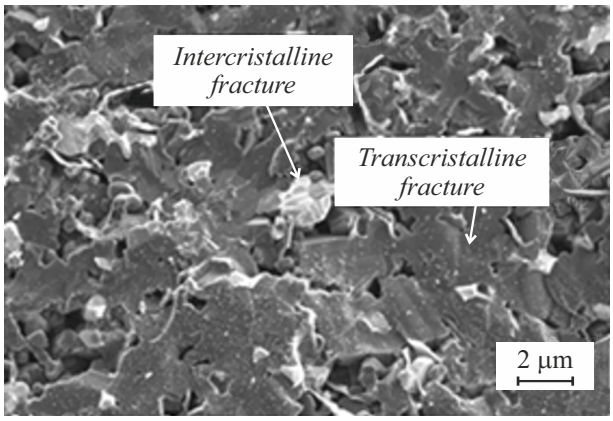


Figure 5. Fracture surface of sample T10sHP.

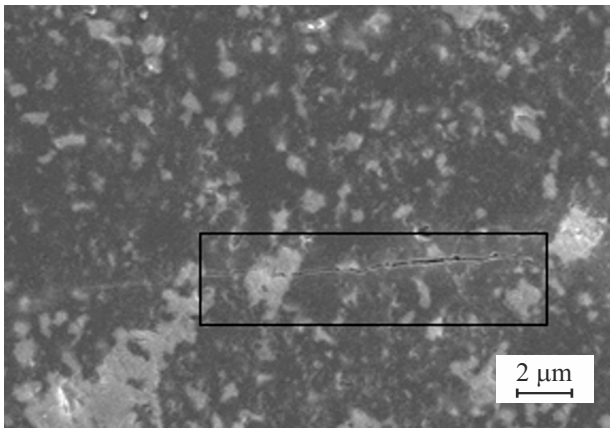


Figure 6. Fracture propagation in the ceramics volume.

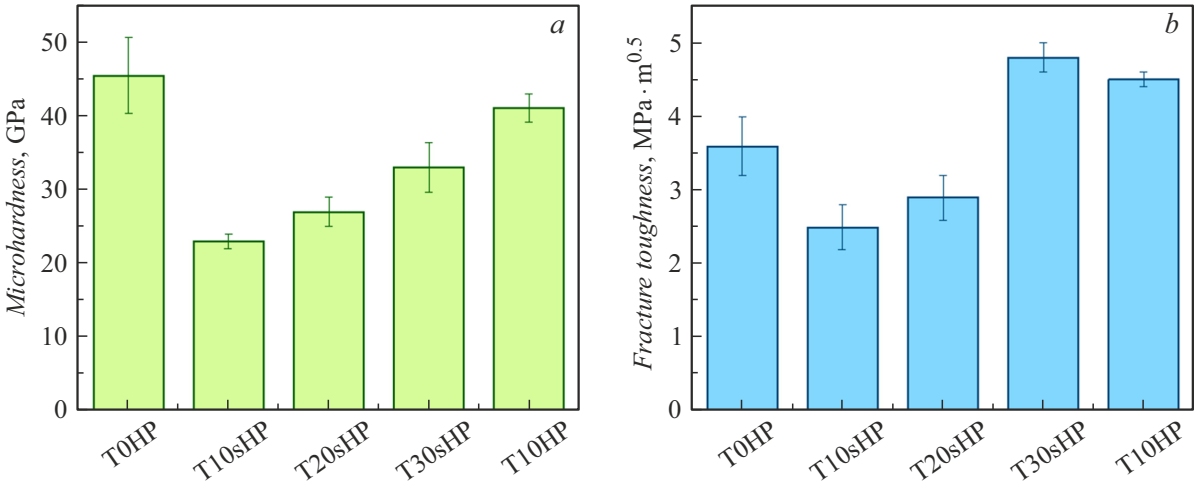


Figure 7. Microhardness (*a*) and fracture toughness (*b*) of the B_4C/TiB_2 composite ceramics.

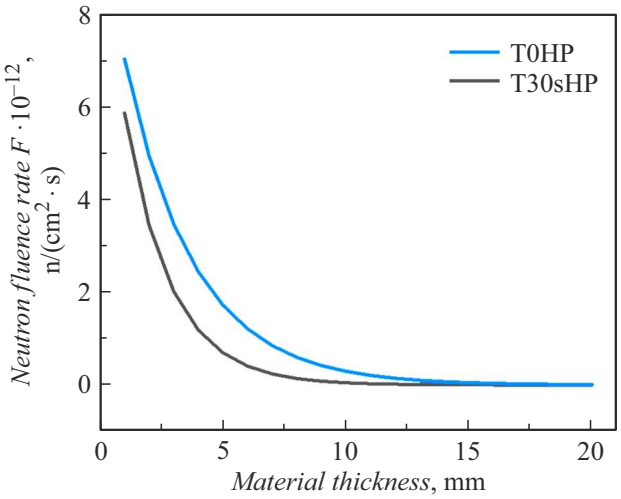


Figure 8. Dependence of the thermal neutron flux on the thickness of samples T0HP and T30sHP.

introduction of 30 mol% titanium diboride additive into the absorbing material will make it possible to increase its absorbing capacity by a factor of 4.3.

Conclusion

B_4C/TiB_2 composite ceramics was made by the boron carbide reduction technique. Compaction of the pre-synthesized B_4C/TiB_2 mixture was performed and the synthesis and pressing processes were combined. It was found that the relative density of ceramics increased with the fraction of TiB_2 . However, for compaction of the pre-synthesized batch to make a composite material with the relative density higher than that of pure B_4C, 30 mol% TiB_2 additive shall be introduced. Simultaneous synthesis and hot pressing as early as at a relatively low content of TiB_2 (10 mol%) makes it possible to fabricate a high-density material (relative density 99.90%) with evenly distributed diboride grains. Such ceramics is characterized by high microhardness 41.1 GPa and fracture toughness 4.5 MPa · $m^{0.5}$. Note also that the introduction of 30 mol% titanium diboride additive into the boron carbide ceramics makes it possible to increase the material's absorbing capacity by a factor of ~ 4.3.

Funding

The study was carried out in accordance with the state assignment of the Ministry of Science and Higher Education (Code FSUN-2023-0008).

Conflict of interest

The authors declare no conflict of interest.

References

[1] W.S. Rubink, V. Ageh, H. Lide, N.A. Ley, M.L. Young, D.T. Casem, E.J. Faierson, T.W. Scharf. J. Eur. Ceram. Soc., **41** (1), 3321 (2021). DOI: 10.1016/j.jeurceramsoc.2021.01.044
[2] I.J. Shon. Ceram. Int., **42** (16), 19406 (2016). DOI: 10.1016/j.ceramint.2016.08.132
[3] R.M. White, E.C. Dickey. J. Eur. Ceram. Soc., **34** (9), 2043 (2014). DOI: 10.1016/j.jeurceramsoc.2013.08.012
[4] D.V. Dik, T.S. Gudyma, A.A. Filippov, V.M. Fomin, Yu.L. Krutsky. Prikladnaya mekhanika i tekhnicheskaya fisika, **2** (81), 2024 (2020) (in Russian). DOI: 10.15372/PMTF202315362
[5] R. He, L. Jing, Z. Qu, Z. Zhou, S. Ai, W. Kai. Mater. Des., **71**, 56 (2015). DOI: 10.1016/j.matdes.2015.01.002
[6] J.D. Clayton, J. Rodriguez, T.W. Scharf, C.L. Williams. J. Eur. Ceram. Soc., **41** (6), 3321 (2021). DOI: 10.1016/j.jeurceramsoc.2021.01.044

[7] O. Coban, M. Bugdayci, M.E. Acma. J. Australian Ceram. Soc., **58**, 777 (2022). DOI: 10.1007/s41779-022-00714-5
[8] P. Svec, L. Čaplovič. Process. Appl. Ceram., **16** (4), 358 (2022). DOI: 10.2298/PAC2204358S
[9] Y.L. Krutskii, N.Y. Cherkasova, T.S. Gudyma, O.V. Netskina, T.M. Krutskaya. Izv. Ferr. Metall., **51** (2), 93 (2021). DOI: 10.3103/S0967091221020029
[10] T.S.R.C. Murthy, B. Basu, R. Balasubramaniam, A.K. Suri, C. Subramanian, R.K. Fotedar. J. Am. Ceram. Soc., **89** (1), 131 (2006). DOI: 10.1111/j.1551-2916.2005.00652.x
[11] S. Failla, C. Melandri, L. Zoli, G. Zucca, D. Sciti. J. Eur. Ceram. Soc., **38** (9), 3089 (2018). DOI: 10.1016/j.jeurceramsoc.2018.02.041
[12] S.G. Huang, K. Vanmeensel, O.J.A. Malek, O. Van der Biest, J. Vleugels. Mater. Sci. Eng., **528** (3), 1302 (2011). DOI: 10.1016/j.msea.2010.10.022
[13] Y. Liu, Z. Li, Y. Peng, Y. Huang, Z. Huang, D. Zhang. Mater. Today Commun., **23**, 100875 (2020). DOI: 10.1016/j.mtcomm.2019.100875
[14] T.S. Gudymajbibitem14 Avtoref. kand. diss. (Krasnoyarsk, SFU,2023) (in Russian)
[15] S. Yamada, K. Hirao, Y. Yamauchi, S. Kanzaki. J. Eur. Ceram. Soc., **23** (7), 1123 (2021). DOI: 10.1016/S0955-2219(02)00274-1
[16] D.V. Dudina, D.M. Hulbert, D. Jiang, C. Unuvar, S.J. Cytron, A.K. Mukherjee. J. Mater. Sci., **43** (10), 3569 (2008). DOI: 10.1007/s10853-008-2563-8
[17] Vl.V. Skorokhod, V.D. Krstic. Powder Metall. Met. Ceram., **39** (7), 414 (2000). DOI: 10.1023/A:1026625909365
[18] A.G. Bannov, V.V. Sokolov, K.D. Dyukova, V.V. Shinkarev, A.V. Ukhina, E.A. Maksimovskii, T.M. Krutskaya, G.G. Kuvshinov. Nanotechnol. Russ., **8** (3–4), 191 (2013). DOI: 10.1134/S1995078013020109
[19] P.B. Kurmashov, V.V. Maksimenko, A.G. Bannov, G.G. Kuvshinov. Khimicheskaya tekhnologiya, **10** (2013) (in Russian).
[20] V.A. Shestakov, T.S. Gudyma, Y.L. Krutskii, N.F. Uvarov, A.E. Brester, I.N. Skovorodin. Inorg. Mater., **57** (5), 481 (2021). DOI: 10.1134/S0020168521050083
[21] T.S. Gudyma, Yu.L. Krutsky, E.A. Maksimovsky, N.Yu. Tcherkasova, N.I. Lapekin, T.V. Larina. Izvestiya vuzov. Poroshkovaya metallurgiya i funktsional'nye pokrytiya, **17**, 2 (35) (in Russian) DOI: 10.17073/1997-308X-2023-2-35-45
[22] GOST 2909-2014 *Ogneupory. Metod opredeleniya kazhushcheisya plotnosty, otkrytoi i obshchei poristosti, vodopogloshcheniys* (IPK Izd-vo standartov, M., 2014), s. 7 (in Russian).
[23] GOST 2999-75. *Metally i splavy. Metod izmereniya tverdosty po Vikkersu* (Izd-vo standartov, M., 1987), s. 29 (in Russian).
[24] GOST 2999-75. *Metally i splavy. Metod izmereniya tverdosty po Vikkersu* (IPK Izd-vo standartov, M., 1987), s. 29 (in Russian).
[25] T.Ya. Kosolapova. *Svoistva, poluchenie i primenenie tugoplavkikh soedineny:* sprav.izd. (Metallurgiya, M. (1986), s. 928 (in Russian)
[26] V.K. Rezepov, V.P. Denisov, N.A. Kirilyuk, Yu.G. Dragunov, S.B. Ryzhov. *Reaktory VVER — 1000 dlya atomnykh elektrostantsyi* (NPO „Gidropress“, M., 2004), s. 333 (in Russian).

Translated by E.Ilinskaya